Time-resolved dosimetric verification of respiratory-gated radiotherapy exposures using a high-resolution 2D ionisation chamber array

Time-resolved dosimetric verification of respiratory-gated radiotherapy exposures using a high-resolution 2D ionisation chamber array

2016 Phys. Med. Biol. 61 5529

(http://iopscience.iop.org/0031-9155/61/15/5529)

OPEN ACCESS
IOP Publishing | Institute of Physics and Engineering in Medicine Physics in Medicine & Biology
Phys. Med. Biol. **61** (2016) 5529–5546 doi:10.1088/0031-9155/61/15/5529

Time-resolved dosimetric verification of respiratory-gated radiotherapy exposures using a high-resolution 2D ionisation chamber array

R B King[1], C E Agnew[2], B F O'Connell[2], K M Prise[1], A R Hounsell[1,2] and C K McGarry[1,2]

[1] Centre for Cancer Research and Cell Biology, Queen's University Belfast, Belfast, BT9 7AE, UK
[2] Radiotherapy Physics, Northern Ireland Cancer Centre, Belfast Health and Social Care Trust, Belfast, BT9 7AB, UK

E-mail: r.king@qub.ac.uk

Received 30 March 2016, revised 9 June 2016
Accepted for publication 15 June 2016
Published 6 July 2016

Abstract

The aim of this work was to track and verify the delivery of respiratory-gated irradiations, performed with three versions of TrueBeam linac, using a novel phantom arrangement that combined the OCTAVIUS® SRS 1000 array with a moving platform. The platform was programmed to generate sinusoidal motion of the array. This motion was tracked using the real-time position management (RPM) system and four amplitude gating options were employed to interrupt MV beam delivery when the platform was not located within set limits. Time-resolved spatial information extracted from analysis of x-ray fluences measured by the array was compared to the programmed motion of the platform and to the trace recorded by the RPM system during the delivery of the x-ray field. Temporal data recorded by the phantom and the RPM system were validated against trajectory log files, recorded by the linac during the irradiation, as well as oscilloscope waveforms recorded from the linac target signal. Gamma analysis was employed to compare time-integrated 2D x-ray dose fluences with theoretical fluences derived from the probability density function for each of the gating settings applied, where gamma criteria of 2%/2 mm, 1%/1 mm and 0.5%/0.5 mm were used to evaluate the limitations of the RPM system. Excellent agreement was observed in the analysis of spatial

information extracted from the SRS 1000 array measurements. Comparisons of the average platform position with the expected position indicated absolute deviations of <0.5 mm for all four gating settings. Differences were observed when comparing time-resolved beam-on data stored in the RPM files and trajectory logs to the true target signal waveforms. Trajectory log files underestimated the cycle time between consecutive beam-on windows by 10.0 ± 0.8 ms. All measured fluences achieved 100% pass-rates using gamma criteria of 2%/2 mm and 50% of the fluences achieved pass-rates >90% when criteria of 0.5%/0.5 mm were used. Results using this novel phantom arrangement indicate that the RPM system is capable of accurately gating x-ray exposure during the delivery of a fixed-field treatment beam.

Keywords: time-resolved dosimetry, respiratory gating, treatment verification

S Online supplementary data available from stacks.iop.org/PMB/61/5529/mmedia

(Some figures may appear in colour only in the online journal)

1. Introduction

In recent years a number of new technologies have been introduced into the radiotherapy environment to improve the accuracy of external beam treatments. A large proportion of these tools are aimed at improving the geometric accuracy of individual patient's treatments, with the goals of ensuring accurate dose delivery to the target volume and reducing harmful side-effects from normal tissue toxicity. The introduction of respiratory gating technology is an example of this, where motion of a target volume is tracked, either directly or through the use of a surrogate, and irradiation from the linac is only enabled when set constraints are met (Korreman 2008). The real-time position management™ (RPM) system (Varian Medical Systems, Palo Alto) is a video-based gating system designed to correlate x-ray exposures with the monitored position of an infrared marker block and to interrupt treatment exposures if the respiratory signal is not within set constraints. The RPM system can be incorporated into both imaging and treatment modalities. Studies have therefore been conducted to verify the geometric accuracy of axial CT images correlated to the RPM respiratory signal (Yamamoto *et al* 2008, Nakamura *et al* 2009,O'Connell *et al* 2015), as well as evaluate its effectiveness at reducing respiration-induced treatment uncertainty (Ford *et al* 2002, Berbeco *et al* 2005, Tai *et al* 2010).

The incorporation of gating technology into treatment exposures adds another degree of complexity to the dosimetric verification of treatment delivery. Additional tests are recommended to verify accurate communication between the gating system and the linac control unit and ensure accurate delivery of the planned treatment dose (Keall *et al* 2006). A number of approaches have been suggested for dosimetric quality assurance (QA) of respiratory gated treatments. Radiographic/radiochromic film and ionisation chamber measurements are tools commonly employed to validate new radiotherapy technology and a number of early studies reported positive results using these tools when combined with custom built moving platforms (Kubo *et al* 2000, Hugo *et al* 2002). However, for intensity modulated radiation therapy (IMRT), it was highlighted that the addition of gating to a patient's treatment has the potential

to introduce additional dosimetric errors depending on the method used to modulate the x-ray fluence (Duan *et al* 2003).

Phantom arrangements that incorporate 2D dosimetry arrays have also been proposed for the verification of gated treatments. A prototype device designed by Nelms *et al* (2007) combined the MapCHECK 2D diode array (Sun Nuclear Corporation, Melbourne, FL) with a high-precision programmable platform capable of independent motion in two dimensions. The authors found that the device was effective at quantifying the degradation in dose uniformity that results from a moving target and that it could easily be integrated with the RPM gating system for QA purposes.

More recently, Woods and Rong (2015) published a report on the development of a comprehensive QA program for the testing of the RPM system. This QA scheme employed the CIRS dynamic thoracic phantom (CIRS Inc., Norfolk, VA), together with radiochromic film and optically stimulated luminescence detectors, for 2D fluence and point dose checks. The scheme was tested across 8 TrueBeam linacs (Varian Medical Systems), where the authors also utilised on-board kV and MV-portal imagers to verify the temporal accuracy of the RPM beam-enable gates. Film measurements were found to be within 3% of expected for a 7-field IMRT plan delivered under gating conditions with the phantom moving sinusoidally. Using additional data from other sources (McCabe and Wiersma 2014), the authors estimated the temporal accuracy of the beam-enable gates to be 139 ± 10 ms for MV imaging beams and 92 ± 11 ms for kV beams. These uncertainties are of a similar magnitude to those measured by other groups (e.g. Chang *et al* (2011)), who reported delays of 90 ± 10 ms using gafchromic film for MV beams gated with the RPM system.

An alternative approach to measuring dose distributions is to exploit the log files that are generated by Varian linacs during the delivery of an external beam treatment. The merits of log-file-based dose reconstruction for patient-specific QA of IMRT techniques have previously been reported by a number of groups (Litzenberg *et al* 2002, Agnew *et al* 2012, Sun *et al* 2013). This technique has also been assessed for the purposes of gated-volumetric modulated arc therapy (VMAT) verification (Qian *et al* 2011). Qian *et al* verified the results of the log-file-based reconstructed dose against planar fluences, acquired using a 2D ion chamber array, and observed 93.5–100% gamma agreement between the two techniques using 3%/3 mm criteria.

While many of the reported studies (e.g. Kubo *et al* (2000), Nelms *et al* (2007), Woods and Rong (2015)) have proposed time-integrated techniques to dosimetrically verify gated beam delivery, the time-dependent triggering inherent in these treatments emphasises the need for time-resolved dosimetry to fully validate their delivery. Respiratory gating is typically employed in combination with highly conformal techniques such as VMAT and stereotactic ablative radiotherapy (SABR). These techniques are complex to both plan and to verify the delivery accuracy. Nordström *et al* (2013) highlighted the potential for delivery errors at certain gantry angles to be blurred during integrated verification of VMAT deliveries and recommended the use of time-resolved '4D' dosimetry to evaluate the delivery at the control point level to enable observation of systematic and plan-specific errors. The complexity of these treatment techniques is further exacerbated when motion and gating are included and it is therefore important for gating techniques to be verified independently (to isolate any errors) before evaluating them in combination with VMAT or SABR.

In this report we propose a novel phantom arrangement that enables the acquisition of time-resolved 2D dose fluences from within the patient's frame of reference by combining a high resolution 2D ionisation chamber array (capable of 100 ms temporal resolution) with a programmable moving platform. This phantom arrangement was tested using the RPM system installed on four TrueBeam linacs, where it's time-resolved data was validated against several data sources and its integrated x-ray fluences were compared to expected fluences.

It is expected that the periodic sampling of gated x-ray exposures with this arrangement will enable a more robust validation of gated treatments by evaluating the gated x-ray output in both spatial and temporal domains.

2. Materials and methods

2.1. Dose delivery system

Four TrueBeam linacs, operating with 3 different version iterations (two v1.5, a v1.6 and a v2.0), were studied in this investigation. A single 6 MV x-ray field was used to deliver 200 monitor units (MU) to the phantom arrangement from a static gantry angle. The x-rays were confined to a fixed field size of $4 \times 4\,\mathrm{cm}^2$ and delivered at a nominal dose-rate of 600 MU min^{-1}.

2.2. Gated exposure delivery

Each linac was equipped with the RPM system which is composed of a ceiling mounted stereo camera, enclosing two detectors each surrounded by an array of infrared light-emitting diodes (LEDs). The LEDs illuminate a marker block, containing four reflective markers, placed on the patient's surface. The markers reflect the infrared light onto the stereo camera allowing its position to be tracked at a frequency of 30 Hz, along the three Cartesian axes. The tracking signal is interpreted by a workstation that is capable of invoking different gating options including amplitude and phase-based gating. When the position of the marker block is outside the constraints set on the workstation a beam-disable (beam-hold) gate is exerted on the linac radiation output.

The amplitude gating constraints used throughout this investigation are illustrated as a schematic in figure 1(a) for a sinusoidal oscillation of 2.5 cm amplitude. Four different amplitude constraints were used to gate the radiation output from the linac so that it was only enabled when the phantom was within $\pm 30\%$ and $\pm 20\%$ of its central position (gating settings *A* and *B* respectively), and at each 20% extreme of its motion (i.e. end inspiration and end expiration, gating settings *C* and *D* respectively). Exposures without gating were also performed for each breathing period and an additional exposure was carried out on each TrueBeam when the phantom was static with the detector aligned along the linac isocentre.

2.3. Acquisition arrangement

A schematic of the experimental arrangement used to acquire time resolved 2D dose fluences during the irradiations is displayed in figure 1(b) adjacent to a photograph of the arrangement in figure 1(c). The moving platform used in this investigation has been described previously (Chinneck *et al* 2010, Cole *et al* 2012) and is based on a design originally described by Dietrich *et al* (2005). The motion of the platform is controlled through the use of machined disks that recreate different breathing patterns. In this investigation a sinusoidal oscillation with a peak-to-trough amplitude of 2.5 cm was used for all irradiations. The oscillation period of the platform can be adjusted using an analogue control. Studies elsewhere have reported that the typical breathing cycle for a healthy individual has a period of approximately 4 s (range 2.7–6.6 s, Seppenwoolde *et al* 2002). Therefore, breathing periods of 3, 4 and 6 s were chosen to represent a typical range of periods.

The Varian RPM four point reflector block was positioned on a shelf attached to the moving platform so that it could be observed within the field of view of the RPM detection system.

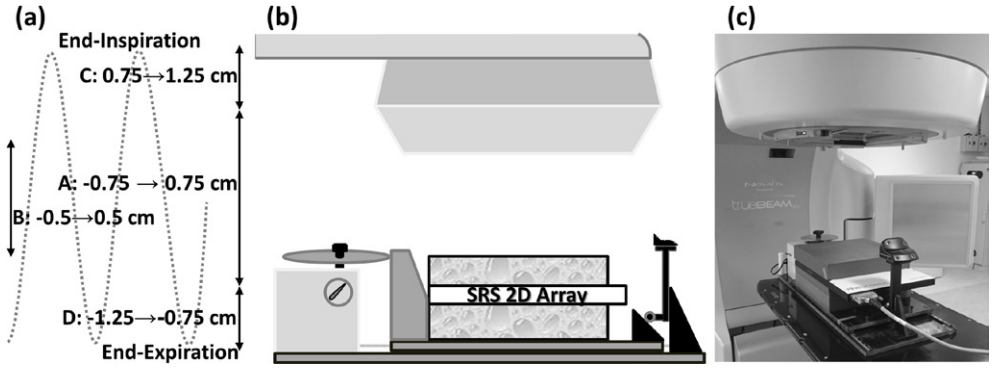

Figure 1. Experimental arrangement. (a) Schematic indicating the amplitude gating constraints applied to a 2.5 cm sinusoidal oscillation. (b) Schematic illustrating the position of the OCTAVIUS SRS array on the programmable moving platform. (c) Photograph of the phantom arrangement positioned below the treatment head of a TrueBeam linac.

The shelf was mounted such that it moved across a 45° wedge, relative to the platform surface. This resulted in vertical translations of the shelf that were synchronised with the horizontal motion of the platform and were of the same amplitude.

2.3.1. OCTAVIUS SRS array. The OCTAVIUS® SRS 1000 array (PTW, Freiburg, Germany) was positioned on the moving platform so that its detection plane was aligned with the isocentre of the linac, with 5 cm of WTe solid water material (Barts and The London NHS Trust, London, UK) placed above and below the detector to act as build-up and backscatter material respectively. The 2D array consists of 977 liquid-filled ionization chambers distributed across a square active detection region of area $11 \times 11\,cm^2$, with variable detector spacing across this area. The maximum physical resolution of the array is 2.5 mm which is achieved over an area of $5 \times 5\,cm^2$ within its central region and along the primary orthogonal axis. The remaining area within the detection region is sampled by chambers that are distributed with a checkerboard pattern. Verisoft v6.2 acquisition and analysis software (PTW) was used to acquire time-resolved 2D fluences of the dose with a temporal resolution of 100 ms.

2.3.2. Linac target signal tracking. To provide additional data on the dosimetric output of the linac during the irradiations, an oscilloscope was used to probe the TrueBeam digital output of the linac target current.

2.3.3. RPM data. Following each gated irradiation, the offline review program (Varian Medical Systems) was used to examine the motion traces recorded by the RPM system. The data presented in offline review includes a temporal trace of the motion interpreted from the RPM camera system, the set amplitude constraints and gates to indicate the time periods when the trace is within the set gating parameters. The recorded data for each of the gated exposures were exported (via Aria version 11) as tab-delimited txt files with an interpolated sampling rate of 67 Hz, and imported into MATLAB V.7.10.0 (MathWorks, Natick, MA) to allow comparison with the other sources of time-resolved data.

2.3.4. Trajectory logs. Trajectory log files recorded during the irradiations were analysed using in-house software written in MATLAB (Agnew *et al* 2014). During each clinical

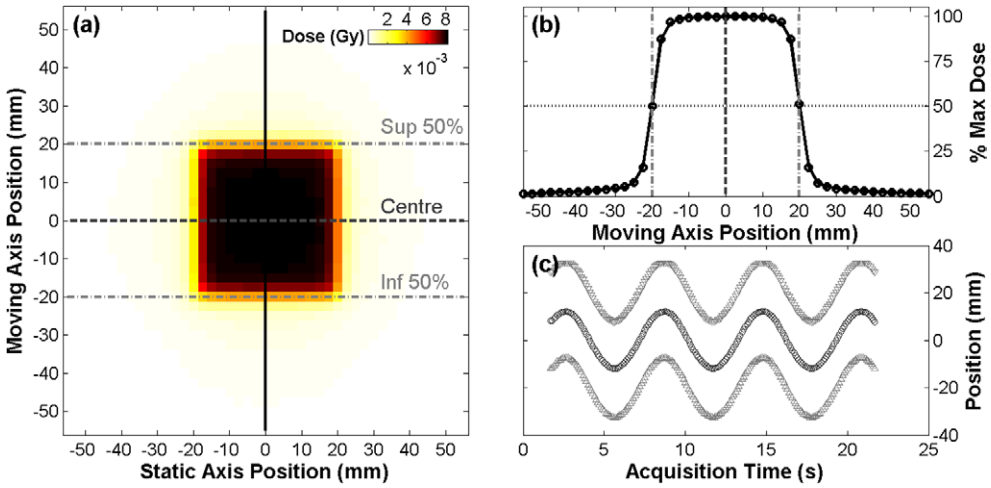

Figure 2. Analysis of time-resolved 2D dose fluences. (a) Example 2D dose fluence. Solid vertical line indicates plane used to derive 1D profile of the variation of dose across the area of the detector. (b) Profile taken along the sample plane. (c) Time-resolved plots of variation in location of the three reference points during an exposure when the platform oscillated with a period of 6 s. Colour available online only.

irradiation the console of the TrueBeam linac will record data every 20 ms to a single trajectory log file. A detailed description on the information recorded within these log files can be obtained from Varian (Varian Medical Systems 2011, 2013).

2.4. Temporal and spatial analysis of time-resolved data

The Verisoft output files were imported into MATLAB for analysis. An example of a 2D fluence measured during a 100 ms time interval is displayed in figure 2(a). For each 2D acquisition a 1D profile was taken through the dose fluence along the central axis of the array, parallel to the direction of the platform's motion (figure 2(b)). The superior and inferior coordinates where the dose was 50% of the maximum (dash-dot grey lines in figure 2) were determined to an interpolated resolution of 0.25 mm. The centre of the spatial profile was determined from the average of these coordinates (dashed line), and used to track the motion of the dose profile across the SRS array.

Figure 2(c) displays an example of how these three points varied over time for a continuous exposure using a 6 s breathing period. Analysis was performed on the SRS array-generated time-resolved traces for each gating condition and breathing period for the four TrueBeam linacs. The mean and standard deviation of the spatial coordinates extracted over the entire exposure were calculated and compared to that expected for a finitely sampled sinusoidal trace.

As each of the four sources of time-resolved data was recorded on separate workstations, the timestamps of their respective data samples were not synchronised and it was necessary to determine appropriate delays between the individual datasets. Although the target signal was considered the ground truth throughout this investigation, the RPM data was used to synchronise each of the data sources as they included both spatial data and gates to indicate when set amplitude constraints were met. For SRS array measurements, the time-resolved spatial profiles were compared to the marker block position traces recorded by the RPM system. The data recorded by the two data sources during the first beam-on period (i.e. first exposure

segment) were compared and a temporal delay was introduced into the SRS array data to achieve the best agreement.

To derive a suitable correction factor for the target signal and trajectory log datasets, the RPM beam-disable gate corresponding to the deactivation of the first segment was selected as the reference to compare to the RPM data. A delay was introduced to the time axis of both the trajectory log files and the target signal data so that the first segment's beam-off flag occurred at the same time for the three data sources. While the SRS array and target signal data were recorded on independent workstations, the trajectory log files were generated by a Varian workstation that communicates with the RPM system. The delay term derived from comparing these two data sources therefore effectively indicated a delay in the automatic commencement of digital recording by the RPM and linac control systems.

Further analysis was performed to ensure that the four data sources remained synchronised throughout each gated exposure. Beam-on flags interpreted from the target signal were used as the ground truth reference to compare to the other data sources. The time difference (Δt) between the reference signal beam-on flag (t_{ref}) and the beam-on/beam-enable times from the three additional data sources (t_x) were then determined for each segment (i) (i.e. $\Delta t(i) = t_x(i) - t_{\text{ref}}(i)$). Negative values of Δt indicated that the gates/flags in the analysed signal occurred before the corresponding flags in the reference signal, while positive values indicated that the analysed signal was delayed with respect to the reference signal.

2.5. Gamma analysis

Gamma analysis was also employed to verify accurate delivery of the gated exposures. Using the technique described by Foster *et al* (2015), theoretically expected 2D dose fluences were generated by convolving a dose fluence, measured during an exposure when the SRS array was stationary, with the probability density function (PDF) of a 2.5 cm sinusoidal oscillation, confined to the same amplitude limits as the set constraints used in this investigation.

MATLAB was used to calculate the convolution of the static 2D fluence with the PDF of the expected gated motion and generate a theoretical 2D fluence for the gated acquisition. Verisoft was used to perform gamma analysis between the measured and theoretical dose distributions for each of the motion periods and gating settings, where a range of gamma criteria (2%/2 mm, 1%/1 mm and 0.5%/0.5 mm) were used to assess the limitations of the gating modality.

3. Results

Figure 3 displays results from the four data sources for a gated exposure performed on a TrueBeam version 2.0. In this example the moving platform oscillated with a period of 4 s and RPM beam-enable amplitude gating constraints of 0.75 cm and 1.25 cm (i.e. end inspiration, gating setting *C*) were applied to the exposure. The time-resolved trace extracted from the SRS array data (black data points figures 3(a)–(c)) corresponds to the motion of the centre of the measured dose profile. For this acquisition the SRS array trace is observed to agree well with the measured RPM trace of the phantom motion (dashed grey line). The amplitude constraints are also indicated on this figure by the dashed horizontal lines and the RPM-determined beam-enable/disable gates corresponding to the platform position satisfying these constraints are overlaid as vertical dotted and dash-dotted lines respectively.

The solid grey bars in figures 3(d)–(f) indicate trains of individual pulses generated at a frequency of 360 Hz at the linac target during each irradiation segment. To summarise this

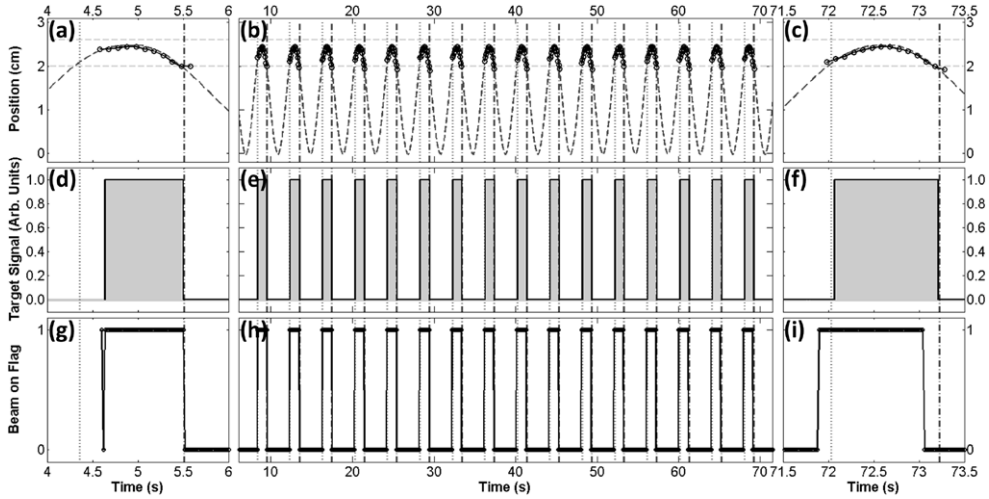

Figure 3. Time-resolved data acquired by RPM system during a gated exposure compared to each of the other data sources. (a)–(c) Saved RPM trace (dark grey) compared to trace derived from SRS array measurements (black). (d)–(f) Measured target signal waveform. (g)–(i) Trajectory log file beam-on/off flags. (a), (d) and (g) correspond to the first radiation segment, (c), (f) and (i) correspond to the last segment and (b), (e) and (h) display data acquired in the intervening period. RPM beam enable/disable gates are indicated in each plot by vertical dotted and dash-dot lines, respectively.

pulse train data, the timing of the initiation of the first pulse and the termination of last pulse for each segment was extracted to indicate beam-on/beam-off flags respectively. The results derived from this analysis are overlaid in the three plots (d)–(f) as a solid line.

The trajectory log data (figures 3(g)–(i)) indicate the beam-on status recorded in the log file in binary format. As no actual time information is logged in the trajectory log files, a 20 ms sampling interval (as defined in the trajectory log file specification (Varian Medical Systems 2011, 2013)) has been assumed. The delay introduced to the trajectory log data to match the termination of the first exposure segment to the corresponding RPM beam-disable gate was observed to be very consistent for all the gated exposures investigated. TrueBeam version 2.0 was observed to produce the most consistent log-file to RPM delay, with a mean of 4.623 s and a standard deviation of 0.019 s for the 12 gated exposures performed using this linac. The average delay for TrueBeam versions 1.5 and 1.6 were found to be very similar to this (4.614 ± 0.136 s and 4.578 ± 0.144 s respectively), albeit with a larger variation in the delay required for individual gated acquisitions. Additional time-resolved plots acquired using this arrangement on a TrueBeam v1.5 and the TrueBeam v2.0 are provided in appendix A of the supplementary material (stacks.iop.org/PMB/61/5529/mmedia).

3.1. OCTAVIUS SRS array spatial data

An average of 239 ± 28 beam-on samples were recorded by the SRS array for each gated exposure. These were analysed to determine the average position of the centre of the dose profile for the gating setting used. The mean positions were compared to the expected values of 0.0 mm for ungated exposures and gating settings *A* and *B* and ± 10.77 mm for the end inspiration/expiration constraints (settings *C* or *D*). Table 1 reports the results of this analysis for

Table 1. Absolute difference between measured and expected mean spatial position of gated SRS array traces.

	Absolute difference (mm) for each gating setting and breathing period (s)														
	No gating			*A*			*B*			*C*			*D*		
Linac	3	4	6	3	4	6	3	4	6	3	4	6	3	4	6
TB v1.5 (I)	0.18	0.01	0.03	0.20	0.27	0.33	0.18	0.09	0.19	0.27	0.23	0.20	0.32	0.28	0.28
TB v1.5 (II)	0.18	0.09	0.02	0.08	0.12	0.39	0.06	0.13	0.16	0.33	0.28	0.31	0.42	0.37	0.28
TB v1.6	0.16	0.08	0.10	0.16	0.04	0.17	0.09	0.12	0.11	0.26	0.19	0.16	0.40	0.37	0.22
TB v2.0	0.02	0.08	0.01	0.24	0.12	0.37	0.13	0.20	0.10	0.33	0.12	0.07	0.36	0.42	0.34

the 12 ungated exposures and 48 gated exposures carried out in this investigation. The maximum absolute difference between the average measured and expected spatial position was 0.42 mm for a 3 s oscillation irradiated using gating setting *D* (end expiration) by a TrueBeam v1.5. However, no apparent trends were observed in the calculated absolute differences with TrueBeam version, gating setting or breathing period applied during the exposure.

3.2. Phase consistency between data sources

It is apparent in figures 3(h) and (i) that the RPM beam-enable gates and trajectory log beam-on flags do not remain synchronised throughout the entire exposure. In this example an accrued time delay of 130 ms was observed between the trajectory log beam-on flag and the RPM beam-enable gate for the last exposure segment. Analysis was therefore performed to determine the time differences between each of the data sources, as described in section 2.4. In this analysis, beam-on flags interpreted from the target signal for each segment were used as the ground truth reference with which to compare corresponding beam-on/-enable flags/gates recorded by the SRS array, trajectory logs and RPM files. The results of this analysis are displayed as colour plots in figure 4 for gated exposures performed on the three versions of TrueBeam studied in this investigation. The colour scale used in the plots (available online) indicates the magnitude and direction of accumulated time differences between the three data sources and the reference target signal. Blue indicates that the beam-on time from the analysed data signal occurred before the corresponding beam-on time in the reference target signal, while red indicates that the analysed signal was delayed with respect to the reference.

The plots in figure 4 also illustrate how the total number of segments required to deliver 200 MU varied as a function of both the gating constraints and the phantom oscillation period. The duration of the time window defining when particular gating constraints were satisfied decreased as the phantom breathing period increased. As a result, a larger number of segments were required when the fastest oscillation period of 3 s was used. The sinusoidal motion of the phantom also meant that the total number of segments for each irradiation was dependent on the gating constraints used. Gating on the end inspiration or end expiration (settings *C* and *D*) required fewer segments to perform the exposure as these both corresponded to a duty cycle of 29.5% of an oscillation period, compared to 20.5% and 13.1% for settings *A* and *B* respectively.

Reviewing trends in the individual plots, good agreement was observed between the SRS array data and target signal data (figures 4(a)–(c)), as indicated by the predominantly green colour plots. The maximum discrepancy between these two data sources was 108 ms which is of a similar magnitude to the SRS array sampling temporal resolution (100 ms). A systematic trend was observed in the comparison between the trajectory log data and the target signal data (figures 4(d)–(f)). The increasing blue trend indicates that the trajectory log beam-on flags occurred prior to the corresponding target signal beam-on times, with the magnitude of the time difference increasing with each successive segment. This trend appeared to be consistent for all three versions of TrueBeam linac. An intermittent difference was also observed for a number of exposures when the RPM beam-enable gates were compared to the target signal beam-on flags (figures 4(g)–(i)). For versions 1.5 and 1.6 of TrueBeam there were a number of exposures where the RPM beam-enable gates occurred at an earlier time compared to the reference beam-on flags. The time difference between the two data sources was also found to increase between successive segments for these exposures. Additional time-resolved data acquired from all data sources is included in appendix A for a selection of the v1.5 (I) and v2.0 exposures for comparison.

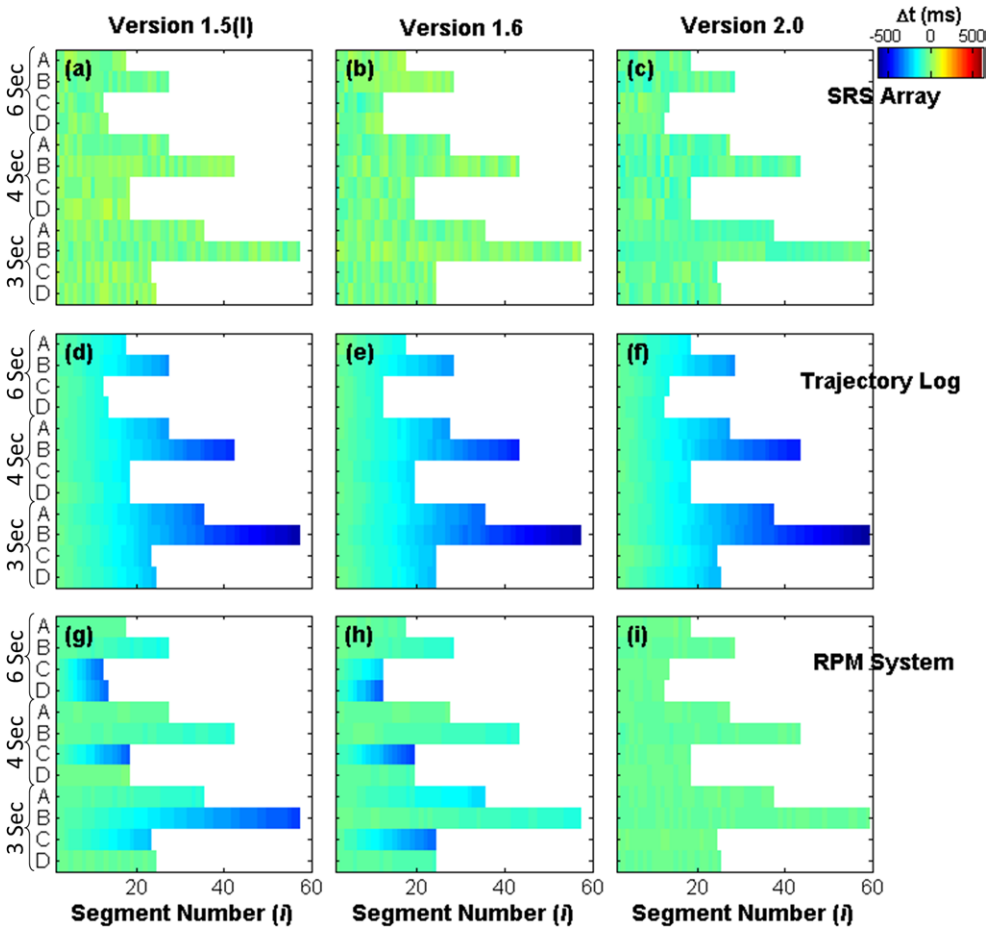

Figure 4. Time difference (Δt) between target signal segment beam-on time and beam-on/beam-enable time recorded by SRS array (a)–(c), trajectory logs (d)–(f) and the RPM system (g)–(i) for the three versions of TrueBeam linac. *Y*-axes of each plot indicate breathing period and gating setting described in figure 1(a). Colour available online only.

To provide a quantifiable evaluation of the discrepancies observed between these data sources, the differences between the times recorded for the start of the last segment (N) of each gated exposure are reported in table 2. For this analysis the target signal beam-on flag time continued to be used as ground truth reference with which the log file's beam-on flag and RPM beam-enable gate were compared. A large amount of variation is observed in the RPM delays for the two v1.5 TrueBeams and the v1.6 TrueBeam. The largest time difference observed for these three linacs was −402 ms indicating that the last RPM beam-enable gate for this exposure occurred 402 ms before the beam-on flag interpreted from the target signal reference. Due to this intermittent discrepancy the average time difference for the 36 gated v1.5 and v1.6 exposures was -192 ± 127 ms. Results for the 12 gated exposures performed on the TrueBeam v2.0 linac were more consistent, resulting in a smaller average and variation in the time differences calculated for this group of exposures (-35 ± 9 ms).

Table 2. Delay between time of last beam-on flag interpreted from oscilloscope target signal waveform and corresponding beam-on/-enable flag recorded in trajectory log file or RPM file for each TrueBeam investigated.

Breathing period (s)	Gate setting	Average total irradiation time (s)	Average number of segments ($N \pm 1$)	Measured difference in last segment beam-on/-enable flag ($\Delta t(N)$, ms)							
				RPM				Log file			
				1.5 (I)	1.5 (II)	1.6	2.0	1.5 (I)	1.5 (II)	1.6	2.0
3	A	53.0	36	−118.5	−62.2	−203.6	−34.7	−360	−380	−340	−380
	B	86.2	58	−396.6	−309.2	−118.3	−38.0	−580	−580	−580	−600
	C	69	24	−249.2	−76.4	−352.1	−29.0	−240	−260	−240	−240
	D	70.4	24	−46.8	−359.0	−79.9	−51.3	−240	−260	−240	−260
4	A	51.8	27	−45.4	−263.4	−37.6	−26.8	−300	−280	−280	−280
	B	83.1	43	−118.1	−305.7	−118.1	−49.4	−420	−440	−440	−440
	C	68.6	18	−354.8	−76.2	−401.9	−47.2	−200	−200	−220	−180
	D	68.6	18	−17.4	−272.7	−64.8	−21.3	−180	−200	−200	−200
6	A	50.3	17	−43.8	−52.6	−60.7	−27.4	−180	−180	−160	−180
	B	80.8	28	−131.4	−112.0	−123.0	−35.3	−300	−300	−300	−300
	C	68.8	13	−347.0	−358.9	−230.4	−29.2	−120	−140	−120	−140
	D	68.9	13	−337.2	−286.5	−363.3	−35.5	−140	−140	−120	−140
			Average	−183.7	−211.2	−179.5	−35.4	−272	−280	−270	−278
			Std. Dev.	137.1	118.3	123.9	9.3	126	125	128	131

Table 2 also illustrates the effects of the systematic trend observed between the linac target signal and the trajectory log data shown in figures 4(d)–(f). While the mean difference between the two data sources was very similar for the 4 linacs (approximately -280 ± 130 ms), there was quite a large variation between the individual exposures for each linac. As previously indicated in figure 4, it is also evident from the table that the difference between the two data sources increased with the number of segments in an exposure, rather than the total irradiation time, with a maximum absolute difference of 600 ms recorded for an exposure consisting of $N = 59$ segments.

3.3. Comparison between target signal and trajectory log data

The cause of the systematic difference between the reference linac target signal and the trajectory log data was investigated further by comparing the beam-on time recorded by both data sources for all segments as well as the time between the activation of consecutive segments. Further information on this analysis can be found in appendix B of the supplementary materials. From the analysis it was observed that the beam-on flags recorded in the trajectory log files consistently overestimated the beam-on period for each segment by 28.58 ± 11.74 ms. However, the trajectory log files also underestimated the time between the activation of consecutive segments by -9.99 ± 8.33 ms. This underestimation of the time between the activation of consecutive segments was the result of the beam-off period between consecutive segments being underestimated in the trajectory log files by 38.57 ± 14.40 ms.

3.4. Gamma analysis

An example of the method used to perform gamma analysis on moving acquisitions is shown in figure 5 for a 4 s breathing period, where no gating was applied to the exposure. Figure 5(a) displays the dose distribution acquired during a static acquisition, this has been convolved with the PDF for a 2.5 cm sinusoidal oscillation that has no amplitude constraints applied (figure 5(b)) to generate the expected 2D dose distribution (figure 5(c)). The resulting gamma distribution from the comparison of the expected dose fluence with the dose fluence that was actually measured (figure 5(d)) is displayed in figure 5(e). Gamma pass criteria of 1% dose difference and 1 mm distance-to-agreement have been used to perform this analysis, with a low dose threshold of 10% and the % dose difference defined relative to the maximum dose. In this example a 100% pass rate was achieved for all pixels.

The same analysis was repeated on all of the gated exposures for each of the four TrueBeams. The results of this analysis are summarised in table 3 for TrueBeam versions 1.5 and 2.0. Gamma analysis using pass criteria of 2%/2 mm was found to yield 100% pass-rates for all exposures, therefore finer gamma criteria of 1%/1 mm and 0.5%/0.5 mm were investigated to identify the limiting criteria. Using gamma criteria of 1%/1 mm only one gated exposure was found to have a pass rate less than 100%. Further analysis of this exposure indicated that the peak dose in the measured fluence was 1.636 Gy, 0.6% higher than the average peak dose (1.626 ± 0.003 Gy). 50% of the measured fluences were observed to achieve pass-rates above 90% when finer criteria of 0.5%/0.5 mm were used.

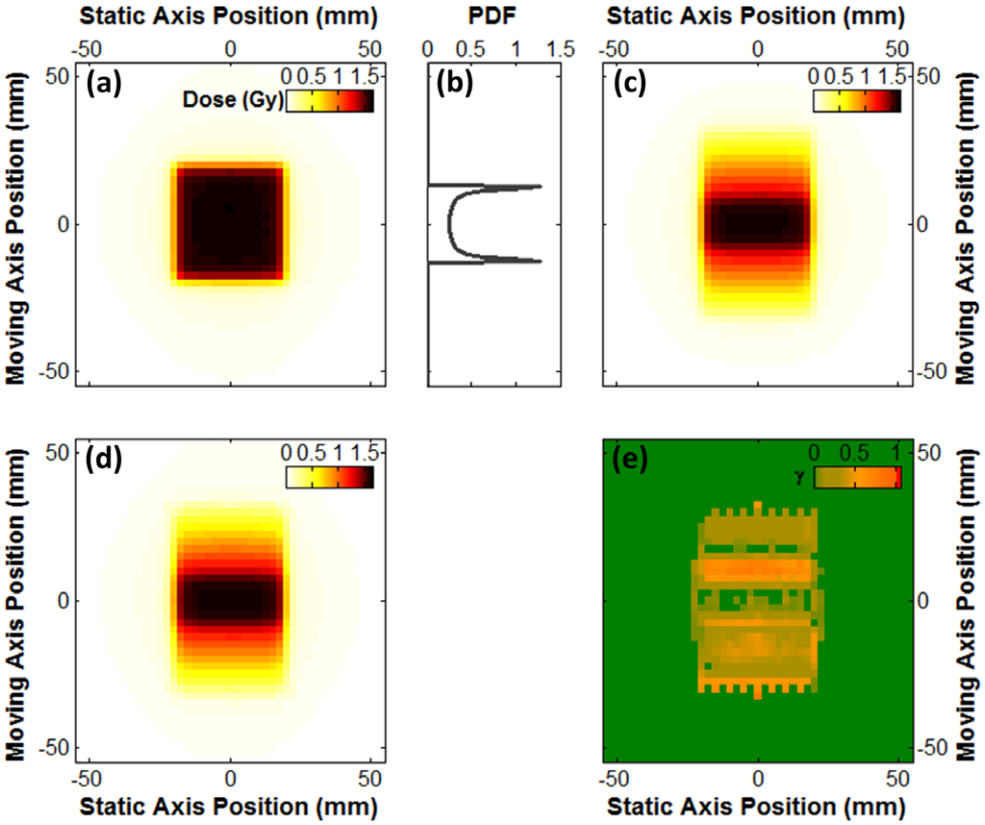

Figure 5. Gamma analysis of integrated dose fluences. (a) 2D dose fluence acquired with SRS array stationary. (b) Expected PDF for 2.5 cm sinusoidal oscillation. (c) Calculated dose distribution resulting from convolution of PDF with static dose fluence. (d) Measured dose fluence when platform oscillated with period of 4 s and no gating was applied to exposure. (e) Results of gamma analysis comparing the two 2D dose fluences.

4. Discussion

4.1. Geometric and dosimetric accuracy

This study used a novel acquisition arrangement, where the OCTAVIUS SRS 1000 2D array was combined with a moving platform, to enable time-resolved dose fluence measurements from a moving frame of reference. This arrangement allowed assessment of the geometric and dosimetric accuracy of the Varian RPM system installed on four TrueBeam linacs under a range of gating conditions and breathing periods. The asymmetry observed in the temporal trace derived from the SRS array analysis displayed in figure 3 indicated a short delay between the RPM gating constraints being met and the linac exposure being activated/deactivated. This asymmetry was observed in the analysis of all the gated exposures and the presence of a time delay agrees with another study (McCabe and Wiersma 2014) that reported an average of 14 ms (3–30 ms) delay between the RPM beam-enable gate and the activation of the MV exposure. Analysis of the time-resolved spatial data acquired with this new phantom arrangement

Table 3. Results of gamma analysis comparing expected and measured 2D dose fluences for two TrueBeam models.

Breathing Period (s)	Gating Setting	TrueBeam v1.5 (I)		TrueBeam v2.0	
		1%/1 mm	0.5%/0.5 mm	1%/1 mm	0.5%/0.5 mm
3	A	100	86.4	100.0	88.9
	B	100	100.0	100.0	100.0
	C	100	94.0	100.0	100.0
	D	100	85.6	100.0	90.4
4	A	100	92.8	100.0	93.7
	B	100	100.0	100.0	95.5
	C	100	87.1	100.0	93.3
	D	100	60.5	100.0	95.1
6	A	100	85.0	100.0	85.3
	B	91.9	48.2	100.0	77.8
	C	100	89.6	100.0	81.4
	D	100	69.3	100.0	92.0

suggested that the effect of this delay was negligible, as only small differences (<0.42 mm) were observed between the expected and measured average position of the phantom for each of the gating settings.

The breathing periods used throughout this investigation correspond to realistic breathing periods interpreted from the results reported by Seppenwoolde *et al* (2002). For gating setting *B*, these periods are equivalent to average velocities in the range of 1.3–2.5 mm s^{-1}. Woods and Rong (2015) observed a trend in this velocity range, where the delay between gating constraints being met and the activation of the MV exposure varied as a function of the phantom velocity. In their study, the authors observed an increasing delay as the velocity was increased, up to speeds of 5 mm s^{-1}. However, analysis of the results reported here suggests that this velocity-dependent delay did not result in any noticeable differences in the mean position of the phantom position for the three breathing periods investigated.

The accuracy of the RPM system was further validated through the results of the gamma analysis comparing measured and expected dose fluences. All the exposures analysed had 100% pass rates using 2%/2 mm criteria and only one exposure had a pass rate less than a 100% when gamma criteria of 1%/1 mm was used. To provide a like-for-like comparison, this study took into account the blurring of the dose fluence that occurs as a result of the phantom motion during gated segments. However, similar results with gamma criteria of 1%/1 mm were observed by Duan *et al* (2003) when they compared IMRT dose fluences acquired using film during either static or gated acquisitions where a 25% duty cycle was applied.

Analysis of fluences acquired from versions v1.5 and v2.0 of TrueBeam indicated that the limiting gamma criteria, where differences between the expected and measured fluences could be clearly distinguished, were of the order of 0.5%/0.5 mm. This 0.5 mm distance-to-agreement criterion is of a similar magnitude to the absolute differences reported in table 1, although it is noted that these gamma criteria are within the expected measurement uncertainty for this experimental arrangement. To test this analysis, gamma comparisons of fluences acquired under the same gating constraints but with different breathing periods were also performed using pass criteria of 0.5%/0.5 mm. Excellent agreement was found for exposures performed on the same linac under the same setup conditions (average pass rate = 94.1%). The technique was found to be sensitive to different setup conditions between the four linacs

and exposures performed on different days, measured pass rates for this analysis were typically less than 75%. The position uncertainties are similar in magnitude to a clinical study by Ford *et al* (2002) who analysed cine mode portal images to determine the intrafraction motion for two patients receiving gated treatment exposures. From analysis of the cine images, the authors determined that the intrafraction motion during the gated exposures was less than 1.4 mm for both patients. Our results provide further evidence that the RPM system can accurately track the position of the marker block and successfully perform gated x-ray exposures with sub mm resolution.

4.2. Inconsistent data logging

Although the SRS array data indicated that the gating system consistently operated as expected, subsequent analysis found that the RPM software installed on TrueBeam versions 1.5 and 1.6 did not reliably record the correct position trace or beam-enable/disable gates. This intermittent discrepancy in the RPM data was not observed in any of the TrueBeam v2.0 exposures. While the operation of the RPM system was not expected to change between TrueBeam iterations, previous work by our group has highlighted the need to test new versions of clinical software as unexpected changes in their operation can occur (McGarry *et al* 2011). Further evidence that indicated the presence of TrueBeam version-specific changes to the RPM system was the improved consistency in the delay derived to synchronise TrueBeam v2.0 log file data with the RPM-generated data. While Woods and Rong (2015) also evaluated multiple TrueBeam linacs, their report did not include details of the TrueBeam versions investigated and no version-specific trends were described. Therefore, to the best of our knowledge, this is the first study to compare the operation of the RPM system between different iterations of TrueBeam linac using information recorded by multiple data sources.

Analysis of results acquired using this phantom arrangement also highlighted a trend in the beam-on flags recorded in the trajectory log files, which consistently occurred prior to the true target signal. A number of studies have used data contained within linac log files to perform pre-treatment verification of the successful delivery of planned treatments (e.g. Litzenberg *et al* 2002, Agnew *et al* 2012, Sun *et al* 2013) and the timing accuracy of the log data is of particular relevance for verifying gated treatments. Qian *et al* (2011) extended this work to the verification of gated-VMAT treatments where they observed 100% pass rates when comparing dose distributions reconstructed from log files of gated irradiations to planned distributions using conventional gamma criteria of 3%/3 mm. Unlike the current study, Qian *et al* did not correlate the activation of the linac exposure with the position of the respiration phantom. If log files are to be used to verify the delivery of gated treatments then accurate interpretation of the data stored within these log files is paramount. For this analysis to be meaningful a complete understanding of potential trajectory log discrepancies, such as those observed within this study, is essential.

5. Conclusion

This study reports on the development of a moving detector arrangement that enables time-resolved dosimetry for the purpose of verifying the delivery of gated radiotherapy treatments. In this investigation the arrangement was used to evaluate the accuracy of the RPM system during a series of gated irradiation scenarios. The phantom arrangement exposed a number of erroneous trends in the data recorded by the RPM system and in the linac trajectory log files. However, as the 2D array 1%/1 mm gamma pass rates showed, the timing discrepancies in the various linac output files had little to no impact on the accurate delivery of the gated treatment fields.

Acknowledgments

This work was supported by grants from Prostate Cancer UK and the Movember foundation (grant number: CEO13_2-004 (FASTMAN Centre)) and the R & D division of the Public Health Agency (grant number: COM/4965/14). The authors would like to acknowledge constructive discussions held with Dr Mark Grattan and the engineering assistance and expertise provided by the electronic and mechanical workshop staff in the NICC. The authors are also grateful for the additional resources and expertise provided by Dr Jason Greenwood, Centre for Plasma Physics, Queen's University Belfast.

References

Agnew C E, Irvine D M, Hounsell A R and McGarry C K 2014 Improvement in clinical step and shoot intensity modulated radiation therapy delivery accuracy on an integrated linear accelerator control system *Pract. Radiat. Oncol.* **4** 43–9

Agnew C E, King R B, Hounsell A R and McGarry C K 2012 Implementation of phantom-less IMRT delivery verification using Varian DynaLog files and R/V output *Phys. Med. Biol.* **57** 6761–77

Berbeco R I, Neicu T, Rietzel E, Chen G T Y and Jiang S B 2005 A technique for respiratory-gated radiotherapy treatment verification with an EPID in cine mode *Phys. Med. Biol.* **50** 3669–79

Chang Z, Liu T, Cai J, Chen Q, Wang Z and Yin F-F 2011 Evaluation of integrated respiratory gating systems on a Novalis Tx system *J. Appl. Clin. Med. Phys.* **12** 3495

Chinneck C D, McJury M and Hounsell A R 2010 The potential for undertaking slow CT using a modern CT scanner *Br. J. Radiol.* **83** 687–93

Cole A J, McGarry C K, Butterworth K T, Prise K M, O'Sullivan J M and Hounsell A R 2012 Development of a novel experimental model to investigate radiobiological implications of respiratory motion in advanced radiotherapy *Phys. Med. Biol.* **57** N411–20

Dietrich L, Tucking T, Nill S and Oelfke U 2005 Compensation for respiratory motion by gated radiotherapy: an experimental study *Phys. Med. Biol.* **50** 2405–14

Duan J, Shen S, Fiveash J B, Brezovich I A, Popple R A and Pareek R N 2003 Dosimetric effect of respiration-gated beam on IMRT delivery *Med. Phys.* **30** 2241–51

Ford E C, Mageras G S, Yorke E, Rosenzweig K E, Wagma R and Ling C C 2002 Evaluation of respiratory movement during gated radiotherapy using film and electronic portal imaging *Int. J. Radiat. Oncol. Biol. Phys.* **52** 522–31

Foster W K, Osei E, Barnett R 2015 Margin selection to compensate for loss of target dose coverage due to target motion during external-beam radiation therapy of the lung *J. Appl. Clin. Med. Phys.* **16** 5089

Hugo G D, Agazaryan N and Solberg T D 2002 An evaluation of gating window size, delivery method, and composite field dosimetry of respiratory-gated IMRT *Med. Phys.* **29** 2517

Keall P, Vedam S, George R, Bartee C, Siebers J, Lerma F, Weiss E and Chung T 2006 The clinical implementation of respiratory-gated intensity-modulated radiotherapy *Med. Dosim.* **31** 152–62

Korreman S S 2008 Motion in radiotherapy: photon therapy *Phys. Med. Biol.* **57** R161–91

Kubo H D and Wang L 2000 Compatibility of Varian 2100C gated operations with enhanced dynamic wedge and IMRT dose delivery *Med. Phys.* **27** 1732–8

Litzenberg D W, Moran J M and Benedick A F 2002 Verification of dynamic and segmental IMRT delivery by dynamic log file analysis *J. Appl. Clin. Med. Phys.* **3** 63–72

McCabe B and Wiersma R 2014 Respiratory gating quality assurance: a simple method to achieve millisecond temporal resolution *Med. Phys.* **41** 185

McGarry C K, Chinneck C D, O'Toole M M, O'Sullivan J M, Prise K M and Hounsell A R 2011 Assessing software upgrades, plan properties and patient geometry using intensity modulated radiation therapy (IMRT) complexity metrics *Med. Phys.* **38** 2027–34

Nakamura M, Narita Y, Sawada A, Matsugi K, Nakata M, Matsuo Y, Mizowaki T and Hiraoka M 2009 Impact of motion velocity on four-dimensional target volumes: a phantom study *Med. Phys.* **36** 1610–7

Nelms B E, Ehler E, Bragg H and Tomé W A 2007 Quality assurance device for four-dimensional IMRT or SBRT and respiratory gating using patient-specific intrafraction motion kernels *J. Appl. Clin. Med. Phys.* **8** 152–68

Nordström F, af Wetterstedt S and Bäck S Å J 2013 4D dosimetry and its applications to pre-treatment quality control and real-time *in vivo* dosimetry of VMAT treatments *J. Phys.: Conf. Ser.* **444** 012021

O'Connell B F, Irvine D M, Cole A J, Hanna G G and McGarry C K 2015 Optimizing geometric accuracy of four-dimensional CT scans acquired using the wall- and couch-mounted Varian® real-time position management™ camera systems *Br. J. Radiol.* **88** 20140624

Qian J, Xing L, Liu W and Luxton G 2011 Dose verification for respiratory-gated volumetric modulated arc therapy *Phys. Med. Biol.* **56** 4827–38

Seppenwoolde Y, Shirato H, Kitamura K, Shimizu S, van Herk M, Lebesque J V and Miyasaka K 2002 Precise and real-time measurement of 3D tumor motion in lung due to breathing and heartbeat, measured during radiotherapy *Int. J. Radiat. Oncol. Biol. Phys.* **53** 822–34

Sun B, Rangaraj D, Palaniswaamy G, Yaddanapudi S, Wooten O, Yang D, Mutic S and Santanam L 2013 Initial experience with TrueBeam trajectory log files for radiation therapy delivery verification *Pract. Radiat. Oncol.* **3** e199–208

Tai A, Christensen J D, Gore E, Khamene A, Boettger T and Li X A 2010 Gated treatment delivery verification with on-line megavoltage fluoroscopy *Int. J. Radiat. Oncol. Biol. Phys.* **76** 1592–8

Varian Medical Systems 2011 TrueBeam Trajectory Log File Specification 100049068-02 USA

Varian Medical Systems 2013 TrueBeam Trajectory Log File Specification 100049068-03 USA

Woods K and Rong Y 2015 Technical report: TG-142 compliant and comprehensive quality assurance tests for respiratory gating *Med. Phys.* **42** 6488–97

Yamamoto T, Langner U, Loo B W, Shen J and Keall P J 2008 Retrospective analysis of artifacts in four-dimensional CT images of 50 abdominal and thoracic radiotherapy patients *Int. J. Radiat. Oncol. Biol. Phys.* **72** 1250–8